

Jizanpeptins, Cyanobacterial Protease Inhibitors from a *Symploca* sp. Cyanobacterium Collected in the Red Sea

David A. Gallegos,[†] Josep Saurí,[‡] Ryan D. Cohen,[§] Xuemei Wan,[†] Patrick Videau,[⊥] Alec O. Vallota-Eastman,[†] Lamiaa A. Shaala,^{||} Daa T. A. Youssef,[#] R. Thomas Williamson,[§] Gary E. Martin,[§] Benjamin Philmus,[†] Aleksandra E. Sikora,[†] Jane E. Ishmael,[†] and Kerry L. McPhail*[†]

[†]Department of Pharmaceutical Sciences, College of Pharmacy, Oregon State University, Corvallis, Oregon 97331, United States

[‡]Structure Elucidation Group, Process and Analytical Research and Development, Merck & Co., Inc., 33 Avenue Louis Pasteur, Boston, Massachusetts 02115, United States

[§]Structure Elucidation Group, Process and Analytical Research and Development, Merck & Co., Inc., 126 East Lincoln Avenue, Rahway, New Jersey 07065, United States

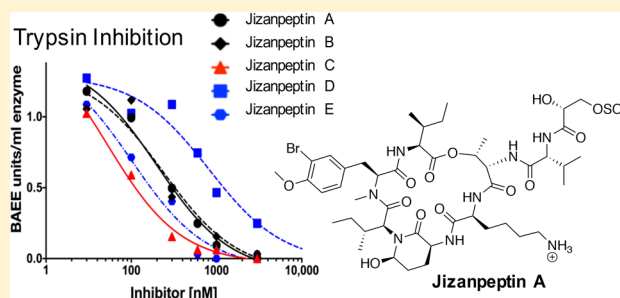
[⊥]Department of Biology, College of Arts and Sciences, Dakota State University, Madison, South Dakota 57042, United States

^{||}Suez Canal University Hospital, Suez Canal University, Ismailia 41522, Egypt

[#]Department of Natural Products, Faculty of Pharmacy, King Abdulaziz University, Jeddah 21589, Saudi Arabia

S Supporting Information

ABSTRACT: Jizanpeptins A–E (1–5) are micropeptin depsipeptides isolated from a Red Sea specimen of a *Symploca* sp. cyanobacterium. The planar structures of the jizanpeptins were established using NMR spectroscopy and mass spectrometry and contain 3-amino-6-hydroxy-2-piperidone (Ahp) as one of eight residues in a typical micropeptin motif, as well as a side chain terminal glyceric acid sulfate moiety. The absolute configurations of the jizanpeptins were assigned using a combination of Marfey's methodology and chiral-phase HPLC analysis of hydrolysis products compared to commercial and synthesized standards. Jizanpeptins A–E showed specific inhibition of the serine protease trypsin ($IC_{50} = 72$ nM to 1 μ M) compared to chymotrypsin ($IC_{50} = 1.4$ to >10 μ M) in vitro and were not overtly cytotoxic to HeLa cervical or NCI-H460 lung cancer cell lines at micromolar concentrations.



Cyanobacteria are prolific producers of biologically active natural products that may act as cytotoxic, neurotoxic, antiparasitic, antiviral, antibacterial, and/or antifungal agents.^{1,2} While the mechanism of action is unknown for many cyanobacterial compounds, common themes include inhibition of cytoskeletal proteins, voltage-gated ion channel modulation, proteases, proteasomes, and enzymes of signal transduction pathways.^{2–4}

There are a substantial number of cyanobacterial natural products reported as protease inhibitors, including the anabaenopeptin, aeruginosin, microginin, microviridin, and micropeptin classes of compounds.² Proteases are ubiquitous enzymes relevant to a variety of metabolic processes in both prokaryotes and eukaryotes and are relevant to diseases ranging from skin⁵ and pulmonary disorders,⁶ to cancer and viral infections,^{7–9} potentially serving as robust therapeutic targets for drug-resistant cells or organisms. In pathogenic bacteria in particular, where many proteases are secreted to facilitate invasion of host tissues, pharmaceutical inhibition of these secreted virulence factors may lead to attenuation of bacterial

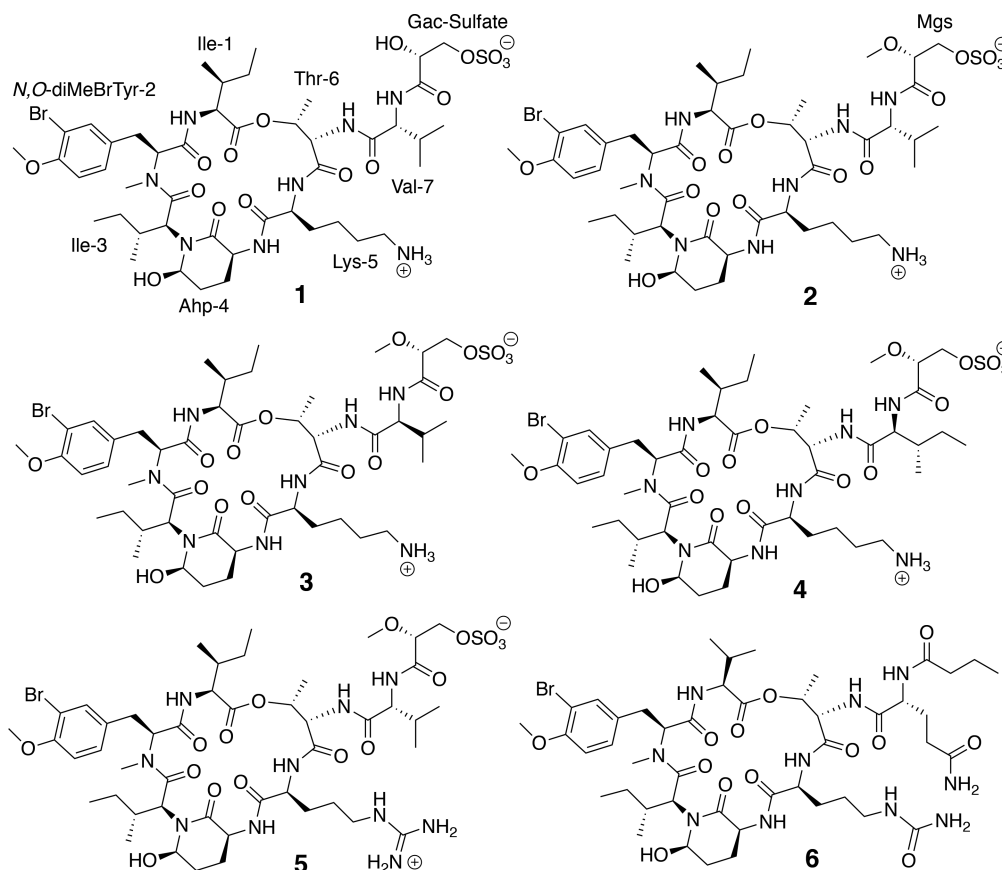
virulence without driving the development of drug resistance observed for compounds that target essential cellular functions.

Freshwater cyanobacteria have yielded a plethora of protease inhibitors, in particular the micropeptin cyclic depsipeptides, while relatively few protease inhibitors have been isolated from marine cyanobacteria. Of the more than 170 depsipeptides that contain Ahp (3-amino-6-hydroxy-2-piperidone), 78% come from freshwater sources, while 20% come from marine and 2% are reported from terrestrial environs (Table S6, Supporting Information). Biologically active natural products reported previously from Red Sea cyanobacteria include the grassypeptolides,¹⁰ apratoxins,¹¹ malyngamide 4,¹² and wewakazole B.¹³ Jizanpeptins A–E (1–5) presented here are the first cyanobacterial protease inhibitors reported from the Red Sea and are the first cyclic depsipeptides containing both bromine and sulfate moieties in this class of compounds. They show differential inhibitory activity between trypsin and chymotryp-

Received: February 4, 2018

Published: May 29, 2018

Chart 1



sin, while displaying little to no cytotoxicity against two human cancer cell lines. These compounds were initially targeted for bioassay-guided isolation due to their inhibition of *Vibrio cholerae* secreted serine protease activity without bactericidal action.

RESULTS AND DISCUSSION

A marine cyanobacterial assemblage dominated by a *Symploca* sp. was collected in 2013 by hand using scuba from the Red Sea, off the coast of Jizan, Saudi Arabia. Phylogenetically, this *Symploca* sp. RS-05/11/13-1 is related to the santacruzamate-producing Panamanian strain¹⁴ and the hoiamide producer from Papua New Guinea¹⁵ (Figure S46, Supporting Information).

The alcohol-preserved tissue was extracted with CH_2Cl_2 -MeOH, and the extract fractionated by automated RP_{18} flash chromatography (Combiflash). The resulting fractions were subjected to a new preliminary biological activity screen to detect inhibition of type II secretion (T2S)-mediated virulence in pathogenic Gram-negative bacteria. This quantitative, high-throughput assay is similar in concept to that reported previously for *Dickeya dadantii*¹⁶ as a model for phytopathogenic bacteria, but uses *Vibrio cholerae* as a model human pathogen, in which the T2S machinery and its cargo proteins are well characterized. Transcriptional activity of T2S, secretion of (or inhibition of secreted) T2S-cargo proteins (e.g., serine proteases VesA, VesB, and VesC¹⁷), and bacterial growth may be assessed simultaneously. The assay relies on cleavage and release of a fluorescent coumarin from the synthetic peptide *N*-tert-butoxycarbonyl-Gln-Ala-Arg-7-amido-4-methylcoumarin, which is commonly employed for monitoring proteolytic

activity of trypsin-like proteases.¹⁷ The serine protease activity can be detected in the medium of growing bacterial cultures and is about 6-fold higher in cultures of wild-type bacteria than in those of a T2S-deficient strain.^{17,18}

One Combiflash fraction (75–100% MeOH) was extremely active (97% reduction in fluorescence) in the T2S-mediated bioassay described above, without affecting bacterial growth. To distinguish whether the active fraction inhibited the cellular T2S machinery itself, secretion of the Ves proteins, or inhibited the activity of secreted serine proteases, the substrate was added to culture supernatants harvested from *V. cholerae*. The active Combiflash fraction indeed inhibited the extracellular serine protease activity, ruling out its potential role in inhibiting T2S. Further fractionation by RP_{18} solid-phase extraction (SPE) and HPLC yielded the pure compounds jizanpeptins A–E (1–5). The small quantities (0.3–1.0 mg) of pure compounds obtained were conserved for structure elucidation by MS and NMR analysis.

Jizanpeptin A (1) yielded a $[\text{M} + \text{NH}_4]^+$ ion at m/z 1122.4391 by HRTOFMS for a molecular formula of $\text{C}_{46}\text{H}_{73}^{79}\text{BrN}_8\text{O}_{16}\text{S}$, with an isotope pattern indicative of a brominated hepta- or octa-depsipeptide incorporating sulfur. The required ammonium bicarbonate buffered MS conditions and the NH_4^+ adduct obtained, as well as the relatively high number of oxygen atoms in the molecular formula, suggested a negatively charged species incorporating a sulfate. The ^1H NMR spectrum for 1 exhibited signals typical for a peptidic cyanobacterial metabolite, including one *N*-methyl singlet (δ_{H} 2.72), five NH signals (δ_{H} 7.50–8.62), seven α -H multiplets (δ_{H} 4.30–5.06), and numerous overlapped methyl doublets (δ_{H} –0.16–1.23, Table 1), as well as an *O*-methyl singlet (δ_{H} 3.77).

Table 1. ¹H NMR Data for Jizanpeptins A–E (1–5) in CDCl₃ (600/800 MHz)

		δ_{H} , mult. (J, Hz)				
unit	position	jizanpeptin A (1)	jizanpeptin B (2)	jizanpeptin C (3)	jizanpeptin D (4)	jizanpeptin E (5)
Ile-1	1					
	2	4.98, dd (9.3, 4.1)	4.97, dd (9.4, 3.7)	4.91, d (3.9)	4.92, m	4.95, m
	3	1.85, m	1.83, m	1.86, m	1.86, m	1.82, m
	4	1.26, 1.13, ^a obs	1.28, 1.12, obs	1.29, 1.12, m	1.27, 1.11, obs	1.27, 1.11, obs
	5	0.91, dd (7.1)	0.91, dd (7.1)	0.91, obs	0.90, t (7.1)	0.90, dd (7.1, obs)
	6	0.70, d (6.9)	0.71, d (6.5)	0.71, d (6.7)	0.70, d (6.3)	0.70, d (6.8)
	NH	7.55, d (9.3)	7.55, d (9.3)	7.55, d (9.3)	7.58, d (9.4)	7.56, d (8.6)
N,O-di-Me-BrTyr	1					
	2	5.06, dd (11.3, 2.6)	5.08, dd (11.3, 2.6)	5.06, dd (11.3, 2.8)	5.06, m	5.06, dd (11.3, 2.6)
	3	3.23, dd (14.4, 11.3)	3.24, obs	3.25, m	3.24, m	3.23, m
		2.80	2.80, dd (14.4, 11.3)	2.79, m	2.78, m	2.79, m
	4					
	5	7.20, dd (8.5, 1.6)	7.20, dd (8.5, 1.6)	7.19, d (7.6)	7.20, dd (8.3, 1.5)	7.20, dd (8.4, 1.4)
	6	7.03, d (8.5)	7.03, d (8.2)	7.03, d (8.1)	7.03, d (8.3)	7.03, d (8.4)
	7					
	8					
	9	7.40, d (1.6)	7.41, d (1.7)	7.40, d (1.7)	7.40, d (1.5)	7.40, d (1.4)
OMe	3.77, s	3.78, s	3.77, s	3.77, s	3.77, s	
NMe	2.72, s	2.73, s	2.72, s	2.72, s	2.72, s	
Ile-2	1					
	2	4.38, d (10.7)	4.39, d (10.3)	4.38, d (10.3)	4.37, d (10.6)	4.37, d (10.6)
	3	1.80, m	1.81, obs	1.79, m	1.79, m	1.79, m
	4	1.11, m	1.11, m	1.12, m	1.10, m	1.12, m
		0.67, m	0.69, obs	0.68, m	0.67, m	0.68, m
	5	0.63, m	0.64, t (14.0, 6.5)	0.63, t (14.2, 6.7)	0.63, m	0.63, m
6	−0.16, d (6.5)	−0.15, d (6.4)	−0.16, d (6.3)	−0.16, d (6.3)	−0.16, d (6.3)	
Ahp	1					
	2	4.45, m	4.46, m	4.45, m	4.45, m	4.45, m
	3	2.53, m	2.54, obs	2.55, m	2.53, m	2.53, m
	4	1.73 1.74, m	1.75, obs 1.74, obs	1.75, obs, 1.76, obs	1.73, m 1.75, m	1.73, m
	5	4.93, bs	4.93, bs	4.93, bs	4.92, bs	4.92, bs
	OH	6.13, bs	6.08, m	6.08, m	6.15, bs	6.16, bs
	NH	7.50, d (8.7)	7.45, d (8.9)	7.44, d (9.2)	7.49, bs	7.51, d (8.9)
Lys/Arg	1					
	2	4.30, bs	4.31, bs	4.30, m	4.28, bs	4.29, bs
	3	2.02, m 1.42	2.01, obs	2.02, m	2.02, 1.43, m	2.02, 1.43, m
	4	1.29, bs	1.25, m	1.23, obs	1.25, bs	1.25, bs
	5	1.49, bs	1.48, m	1.43, m	1.47, bs	3.05, bs
	6	2.74, bs	2.19, bs			
	NH ₃ ⁺					8.43, bs
NH	8.52, d (7.5)	8.49, m	8.47, d (8.8)	8.55, bs	8.73, bs	
Thr	1					
	2	4.60, d (8.7)	4.63, d (8.5)	4.66, d (8.6)	4.69, bs	4.68, d (9.1)
	3	5.50, m	5.49, m	5.49, m	5.49, bs	5.48, m
	4	1.23, obs	1.22, d (6.4)	1.22, d (6.5)	1.20, obs	1.20, obs
NH	8.62, d (8.6)	8.28, bs	8.16, d (9.0)	8.20, bs	8.45, d (8.6)	
Val/Ile-3	1					
	2	4.64, dd (9.1, 5.5)	4.53, dd (8.9, 5.8)	4.39, obs	4.42, bs	4.52, dd (8.9, 7.9)
	3	2.03, obs	2.06, m	2.09, m	1.82, obs	2.05, obs
	4	0.82, d (6.7)	0.85, d (6.7)	0.84, d (6.7)	1.25	0.83, d (6.7)
	5	0.88, d (6.7)	0.89, d (6.6)	0.89, obs	0.85, obs	0.87, d (6.7)
	6				0.83, obs	
NH	7.58, d (9.4)	7.81, d (9.1)	7.76, d (8.6)	7.84, bs	7.77, d (8.9)	
Gac-sulfate/Mgs	1					
	2	4.11, m	3.95, m	3.99, m	3.97, bs	3.95, dd (2.4, 10.5)
	3	4.04, 3.74, dd (10.7, 2.1)	3.99, m 3.75, dd (11.3, 7.7)	3.90, dd (3.3, 10.9), 3.75, dd (11.0, 7.2)	3.87, 3.71, bs	3.92, 3.73, dd (6.7, 2.4)

Table 1. continued

unit	position	δ_{H} , mult. (J, Hz)				
		jizanpeptin A (1)	jizanpeptin B (2)	jizanpeptin C (3)	jizanpeptin D (4)	jizanpeptin E (5)
	OH/ OMe	bs	3.35, obs	3.35, s	3.32, s	3.33, s

^aObs, obscured.

Additional ¹H NMR signals for three oxymethines (δ_{H} 4.11, 4.93, 5.50) and one diastereotopic oxymethylene (δ_{H} 3.74, 4.04), supported by COSY and multiplicity-edited HSQC data, were consistent with the molecular formula in indicating an oxygenated depsipeptide. A substituted tyrosine residue was evident from three nonequivalent, aromatic ¹H NMR signals (δ_{H} 7.03, 7.20, 7.40) accompanied in the HMBC spectrum by ¹³C NMR signals for three methine (δ_{C} 113.3, 130.5, 134.0) and three nonprotonated (δ_{C} 111.4, 131.6, 154.9) aromatic signals (Table 1). HMBC correlations from the *N*-CH₃ singlet to the Tyr α -carbon (δ_{C} 61.0) and from the *O*-CH₃ singlet to a nonprotonated aromatic signal at δ_{C} 154.9 indicated that the tyrosine residue was *N,O*-dimethylated. The additional substituent on this *N,O*-dimethyl Tyr was located adjacent to the *O*-CH₃, in a *meta* position, on the basis of HMBC and COSY data, and was assigned as Br considering the relatively shielded ¹³C NMR shift (δ_{C} 111.4) of the substituted carbon in question. A second atypical amino acid residue was delineated in COSY experiments as a contiguous spin system incorporating an NH (δ_{H} 7.50), a methine (δ_{H} 4.45), and two methylenes (δ_{H} 1.73, 1.74, 2.53) and terminating in an oxymethine (δ_{H} 4.93). HMBC correlations to the same carbonyl ¹³C NMR shift (δ_{C} 169.9) from ¹H NMR signals for both the latter oxymethine and the presumed α -methine were consistent with the presence of a 3-amino-6-hydroxypiperidone (Ahp) residue. At this point, the co-occurrence of the *N,O*-diMe-BrTyr and Ahp moieties led to a comparison of MS and NMR data for **1** with those for symplocamide A,¹⁹ a marine-derived micropeptin previously reported from a Papua New Guinea *Symploca* species. Notable differences in MS and NMR data for jizanpeptin A (**1**, C₄₆H₇₃⁷⁹BrN₈O₁₆S) versus symplocamide A (**6**, C₄₆H₇₂⁷⁹BrN₁₀O₁₃) included the additional SO₃H and two less N atoms for **1**, with no indication of NMR signals for the citrulline or glutamic acid residues found in symplocamide A (**6**). Instead, multiplicity-edited HSQC and COSY data revealed side chain spin systems of the amino acids Ile (two residues), Val, Thr, and Lys (Table S1, Supporting Information). The connectivity of these seven amino acid residues in **1** was delineated by HMBC and ROESY correlations and cyclized through a ring junction Thr, in agreement with the general motif of **6** (Figure 1). The molecular formula for **1** indicated there was an unaccounted C₃H₅O₆S unit, and unassigned 1D NMR signals included a carbonyl carbon (δ_{C} 170.9), an oxymethine (δ_{H} 4.11, δ_{C} 71.6), and an oxymethylene (δ_{H} 4.04, 3.74, δ_{C} 68.9). The latter ¹H and ¹³C NMR signals were interconnected by various COSY and HMBC correlations, and the carbonyl ¹³C NMR signal displayed a correlation from the Val α -H, suggesting *N*-terminal amide formation of the depsipeptide molecule with a terminal glyceric acid (Gac). The remaining sulfate moiety could be appended logically at the primary alcohol, forming a 3-*O*-sulfated glyceric acid moiety (Gac-sulfate), as found in 13 previously reported micropeptins (Table S6, Supporting Information). Thus, the planar macrocyclic structure of

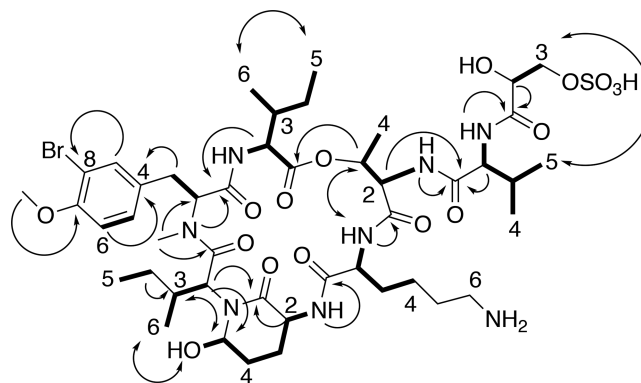


Figure 1. Key 2D NMR correlations for jizanpeptin A (**1**). Bold bonds indicate COSY, single-headed arrows indicate HMBC, and double-headed arrows indicate ROESY correlations.

jizanpeptin A (**1**) was completed (Figure 1, Table S1, Supporting Information).

The planar structures of the other four related depsipeptides, which were purified in workable (although submilligram) quantities, could be assigned by careful inspection and comparison of their characteristically similar MS and NMR data with those for **1**. Jizanpeptins B (**2**) and C (**3**) each exhibited an HRTOFMS ion at m/z 1136.4555 ($[M + \text{NH}_4]^+$) for a molecular formula of C₄₇H₇₅⁷⁹BrN₈O₁₆S, with the additional 14 mass units equating to an additional CH₂ compared to jizanpeptin A (**1**). A second *O*-CH₃ singlet was immediately evident in each of the ¹H NMR spectra for **2** and **3**, which together with a slightly shielded shift of the Gac-sulfate oxymethine multiplet (δ_{H} 4.11 to 3.99), implied a 2-*O*-methylated Gac-sulfate. The latter assignment was corroborated by reciprocal HMBC correlations between the ¹H and ¹³C NMR shifts for the oxymethine and *O*-CH₃ moieties. The identical planar structures for **2** and **3** were confirmed by comprehensive assignment of atom connectivity using COSY, HSQC, HMBC, and ROESY data. However, the specific rotation value for **3** (−37) appeared distinct from those for **1** (−21) and **2** (−18), and 1D chemical shift differences of 0.8–1.4 ppm were apparent for the side chain and northern hemisphere atoms, particularly for α -H and NH of Ile-1, Thr-6, and Val-7 (Table 1, Tables S2 and S3, Supporting Information). These data implied that **2** and **3** varied in configuration at Ile-1, Thr-6, Val-7, or Gac-sulfate, which was subsequently confirmed from Marfey's analysis as described below.

The HRTOFMS $[M + \text{NH}_4]^+$ ion for jizanpeptin D (**4**) at m/z 1150.4679 (C₄₈H₇₇⁷⁹BrN₈O₁₆S) indicated an additional CH₂ group compared to **2** and **3**. The ¹H NMR spectrum for **4** was very similar to those for **2** and **3**, displaying signals for the one *N*-CH₃ and two *O*-CH₃ substituents, with only minor variation detectable in the shielded region that included an additional methylene signal (δ_{H} 1.25). Careful comparison of the chemical shifts and 2D NMR data for the Val, two Ile, Thr, and Lys residues of **2–4** revealed that **4** possesses a third Ile

unit at position 7, replacing the side-chain Val of **2** and **3**, to which the terminal MeGac-sulfate was appended.

Jizanpeptin E (**5**) was found to possess the highest molecular mass with a HRTOFMS $[M + NH_4]^+$ ion at m/z 1164.4596, for a molecular formula of $C_{47}H_{75}^{79}BrN_{10}O_{16}S$. Immediately obvious from the latter was one less C atom than in **4**, and two additional N atoms compared to **1–4**. Although no direct ^{13}C NMR spectrum could be acquired on the small amount of **5** available, analysis of comprehensive 2D NMR data confirmed the presence of the *N,O*-diMe-BrTyr, Ahp, and *O*-Me-Gac-sulfate residues in **5** and led to the assignment of amino acids Ile (two units), Val, Thr, and Arg. The latter Arg in place of the Lys in **1–4** accounted for the additional two N atoms in the molecular formula and was responsible for an additional NH signal (δ_H 8.73), a relatively deshielded methylene proton (δ_H 3.05 for Arg, 2.74 for Lys) and a slightly deshielded ^{13}C NMR shift (δ_C 40.5 for Arg, 39.2 for Lys), deduced from the HSQC spectrum for **5**. As expected, the 2D NMR data for **5** supported a conserved amino acid sequence for the jizanpeptins, incorporating *N,O*-diMe-BrTyr-2, Ahp-4, and Arg-5 in place of Lys-5 in **1–4**.

The absolute configurations of the amino acid units in jizanpeptins A–E (**1–5**) were determined by Marfey's methodology. For each natural product, the acid hydrolysate (0.2 mg, 6 N HCl, 110 °C, overnight) was derivatized with *N*- α -(2,4-dinitro-5-fluorophenyl)-L-leucinamide (L-FDLA, Marfey's reagent) and analyzed by RP₃ or RP₁₈ HPLC comparison with FDLA-derivatized D- and L-amino acid standards. All five jizanpeptins possess the L-configuration for Ile-1, *N,O*-diMe-BrTyr-2, Ahp-4 (after oxidation and comparison to Glu standards) and Thr-6 residues, and L-*allo*-Ile-3. L-Configurations could also be assigned for Lys-5 in jizanpeptins A–D (**1–4**) and for Arg-5 in jizanpeptin E (**5**), as well as for side-chain Val-7 in **3**. In contrast, Val-7 in **1**, **2**, and **5** possess a D-configuration, while Ile-7 in **4** could be assigned as L-Ile. The positions of the L-*allo*-Ile and L-Ile units in **1–5** were assigned by comparison of NMR shifts with other previously described micropeptins, because these residues have been demonstrated to display distinctive, conserved shift differences. The 1H NMR chemical shift values for L-*allo*-Ile at position 1 and L-Ile at position 3 are close matches to micropeptin KB1048, in which L-*allo*-Ile-1 and L-Ile-3 were also assigned.²⁰ The observed shift values were also consistent with those for symprostatis 5, 7, and 10,²¹ including the side chain L-Ile-7, and differed from micropeptin HU1069 (L-Ile-1 and L-Ile-3) shifts.²²

Chiral-phase HPLC analysis was used to determine the absolute configuration of the terminal eighth residue as R-Gac-sulfate in **1**. Specifically, retention times for commercial S- and R-Gac products were compared with Gac in the natural product hydrolysate (Figures S37–S39, Supporting Information) using a Phenomenex Chirex analytical HPLC column with a mobile phase of $CuSO_4-CH_3CN$.

Chiral-phase HPLC was also used to determine the configuration of the side chain terminal 2-*O*-methylated glyceric acid sulfate (Mgs) in jizanpeptins B–E (**2–5**) after synthesis of methylated glyceric acid (Mga) standards following previous literature.¹⁶ The retention times for synthetic R- and S-Mga were compared with Mga detected in the natural product hydrolysate using an analytical Chirobiotic TAG column with a mobile phase of MeOH–NH₄OAc. A match of the natural product hydrolysate components with R-Mga provided an assignment of R-MeGac-sulfate in **2–5**. The 1H NMR chemical shifts for **2–5** were also compared to those for Mgs found at

the same position in reported micropeptins. 1H NMR chemical shifts for oscillapeptin F²³ and symprostatis 5, 7, and 10²¹ closely matched the chemical shifts observed for Mgs in **2–5**.

The *O*-methylated glyceric acid (Mga) moiety has been isolated in many micropeptins. Similarly, many nonmethylated glyceric acid (Gac) moieties have been reported in micropeptins, leading to the question of whether *O*-methylation is an artifact. Reports of Mga-containing micropeptins indicate natural product extraction protocols using 80% MeOH (aq),²³ 50% MeOH(aq),²⁴ 1:1 EtOAc–MeOH,²¹ while those reporting Gac are accompanied by extraction protocols using 7:3 MeOH–H₂O.^{22,25–27} Here we used CH₂Cl₂–MeOH (2:1) as an extraction solvent and obtained both Mga and Gac-containing compounds. There is no apparent correlation between the presence of a methylated glyceric acid and the extraction conditions used, and thus nothing to prompt further investigation of *O*-methylation as an isolation artifact. Lyngbyastatins, planktopeptins, oscillapeptins, largamides, cyanopeptolins, A90720A, micropeptins HU, LH, MM, MZ, and symprostatis all contain glyceric acid (Table S6, Supporting Information). The R-configured Mgs found in the jizanpeptins is also present in the sponge metabolite dysinosin A.²⁸

The *N,O*-diMeBrTyr moiety has been reported in three other micropeptins: kempopeptin B²⁹ and pompanopeptin A,³⁰ both trypsin inhibitors, and the chymotrypsin inhibitor symplocamide A.¹⁹ Lyngbyastatin 10³¹ is an elastase inhibitor, and largamides D, F, and G³² are chymotrypsin inhibitors that each contain N-MeBrTyr. Several other micropeptins contain *N,O*-diMeClTyr (Table S6, Supporting Information).

The structural similarity of **1–5** to cytotoxic micropeptin-like cyclic depsipeptides, together with the protease inhibition activity of the jizanpeptin-containing parent fraction in the T2S-mediated bacterial virulence assay, prompted us to test **1–5** in enzymatic assays for relative inhibition of purified serine proteases trypsin and chymotrypsin, as well as for cytotoxicity to mammalian cells. Jizanpeptins **1–5** displayed a differential pattern of selectivity with 10- to 66-fold greater selectivity for trypsin versus chymotrypsin (Table 2, Figure S47, Supporting

Table 2. Protease Inhibition Activity for Jizanpeptins A–E (1–5)

compound	IC ₅₀ (nM) ± SE (nM)	
	trypsin	chymotrypsin
jizanpeptin A (1)	160 ± 30	>10 000
jizanpeptin B (2)	190 ± 20	>10 000
jizanpeptin C (3)	72 ± 17	1400 ± 700
jizanpeptin D (4)	1000 ± 250	>10 000
jizanpeptin E (5)	150 ± 20	>10 000

Information). The rank order of potencies (in descending order) for inhibition of trypsin activity was **3** > **5** ≥ **1** ≥ **2** > **4**. The most potent trypsin inhibitor, jizanpeptin C (**3**), was the only compound to display full efficacy as a chymotrypsin inhibitor under these standardized assay conditions, with a 19-fold greater potency against trypsin (72 nM) versus chymotrypsin (1.4 μM). None of the jizanpeptins inhibited human NCI-H460 lung (Figure S48, Supporting Information) or HeLa cervical cancer cell viability (Figure S49, Supporting Information), producing no statistically significant change in end-point assays relative to vehicle-treated cells at concentrations up to 3 μM. This lack of activity for **1–5** against the

cancer cell lines tested differs from many cyclic depsipeptide protease inhibitors reported, and the general biological activity profile for 1–5 is in stark contrast to the biological activity profile previously observed for symplocamide A (6).¹⁹ In protease inhibition assays, 6 showed greater selectivity for chymotrypsin over trypsin and was remarkably cytotoxic to NCI-H460 lung cancer cells. Apparent differences in the cytotoxic potential of these protease inhibitors could be attributed to the increased polarity imparted by the terminal Gac-sulfate, which potentially hinders the transport of jizanpeptins into mammalian cells. In support of this hypothesis, dolastatin 13³³ (with a terminal Gac) displayed nanomolar cytotoxicity, while analogues lyngbyastatin 4³⁴ and symplostatin 5²¹ (both with a terminal Gac-sulfate) displayed no cytotoxicity, albeit in different cell lines. Cytotoxicity values are sparsely reported for many of the micropeptides, and those with reported toxicity seem to show no correlation between any singular convergent structural feature (Table S6, Supporting Information). Observed toxicity may be due to nonspecific binding of proteases, as these compounds are proposed to be grazing inhibitors to *Daphnia* in Nature.³⁵

There are several structural features conserved between all Ahp-containing protease inhibitors that are crucial for activity (Table S6, Supporting Information). These include an *N*-methylated *L*-aromatic amino acid at position 2, *L*-Ahp-4, and *L*-Thr-6. Residues at these positions play a critical role in maintaining the correct conformational stability and rigidity.³⁶ Furthermore, the variable side chain originating from *L*-Thr-6 is also necessary for protease activity and is a universal feature in all but one isolated case (micropeptin MZ771).²⁵ The slight structural variations observed among 1–5 allow an SAR comparison between these and published micropeptin-type compounds and determination of a putative “ideal” trypsin inhibitor. The difference between 1 and 2 is a single methylation of OH-2 in Gac, which produces little if any decrease in potency (160 nM ± 30 vs 190 ± 20 nM). Between 2 and 3 there is a change from *D*- to *L*-Val-7 on the pendant side chain and a corresponding increase (nearly 3×) in potency to 72 nM. In comparing 3 and 4, a change from *L*-Val-7 to *L*-Ile-7 is observed, resulting in a large decrease in potency (1000 nM). Jizanpeptin 5 is structurally the same as 2, with *L*-Arg substituted for *L*-Lys. This results in a very slight increase in potency (150 ± 20 nM cf. 190 ± 20 nM, respectively). These SAR results suggest that a side chain *L*-Val-7 is most important for enhanced trypsin-like protease inhibition.

The residue at position 5 (*N*-terminal to Ahp) confers selectivity between proteases. Structures that have position 5 residues with long, polar side chains selectively inhibit trypsin,³⁷ while those with large hydrophobic and aromatic residues like Phe or Leu demonstrate preferential inhibition of chymotrypsin.³⁸ It is notable from Table S6 (Supporting Information) that depsipeptides with polar uncharged side chains (e.g., Gln, Cit, Tyr) also show chymotrypsin selectivity. Thus, the basis for trypsin selectivity may be better articulated as the presence of a polar, charged side chain in the residue at position 5, while a nonpolar or polar uncharged side chain for residue 5 provides chymotrypsin selectivity. Compounds that contain Abu-5 (2-amino-2-butenic acid) are reported to be potent inhibitors of elastase.²¹

There are several trypsin-like serine proteases with relevance to human health involved in diverse biological pathways and diseases that may be good targets for compounds such as the jizanpeptins. In addition to the type II secreted proteases VesA

and VesB of *V. cholerae*, which are involved in activating cholera toxin,^{17,39–42} serine protease autotransporters of Enterobacteriaceae (SPATEs) are present in nearly all pathogenic Enterobacteriaceae.⁴³ Bacterial proteases are particularly promising targets for compounds that may not cross the cell membrane, while also theoretically limiting their potential for negative interactions with host proteases located inside cell membranes. VesA and VesB are also similar to proteases found in the S1A family that comprises mostly eukaryotic proteases including trypsin,⁴⁰ the blood coagulation cascade Factor Xa,⁴⁴ and the kallikreins, which are involved in diverse biological pathways in humans and relevant to neurodegenerative disease⁴⁵ and atopic dermatitis,⁵ for example.

In conclusion, jizanpeptins A–E (1–5) join symplocamide A (6) and a handful of other compounds as depsipeptide protease inhibitors from marine cyanobacteria (Table S6, Supporting Information), although with distinct protease selectivity profiles. Notably, symplocamide A displayed nanomolar activity against NCI-H460 lung cancer cells (IC₅₀ 40 nM) and neuro-2a neuroblastoma cells (IC₅₀ 29 nM).¹⁹ The absence of any significant cytotoxicity to two human cancer cell types for 1–5 presents the opportunity to further investigate their antivirulence potential through inhibition of secreted bacterial trypsin-like proteases and activity against noncancerous cells, pending compound supply via total synthesis or field re-collections.

■ EXPERIMENTAL SECTION

General Experimental Procedures. Optical rotations were measured on a JASCO P-1010 polarimeter. UV data were acquired on a Shimadzu HPLC system equipped with a PDA detector. NMR spectra were acquired on either a Bruker AVANCE 800 with a TXI 5 mm cryoprobe, a Bruker AVANCE III 700 with a ¹³C observe (DCH) cryoprobe, or a 600 MHz Bruker AVANCE III three-channel NMR spectrometer equipped with a TXI 1.7 mm MicroCryoProbe. The residual protonated DMSO solvent peak was used as an internal standard (δ_{H} 2.50, δ_{C} 39.51). HRTOFMS (ES⁺) mass spectra were recorded on an Agilent 6520 Q-TOF mass spectrometer. The isolation of compounds 1–5 and Marfey's and chiral-phase HPLC analyses were conducted on a Shimadzu HPLC system equipped with two LC-20AD pumps and an SPD-M20A photodiode array detector. General reagents were from TCI-America, Sigma-Aldrich Corp., and VWR International.

Collection and Identification. The marine cyanobacterial assemblage (McPhail laboratory voucher number RS-05/11/13-1) was collected in 2013 by hand using scuba (20–26 ft depth) from Ghurab Reef in the Red Sea (N 017°06'38.0", E 042°04'01.9") off the coast of Jizan, Saudi Arabia. The material collected for chemical extraction (1.2 L) was stored in 50% EtOH for transport and then stored at –20 °C until extraction. An aliquot of the field-collected sample (0.5 mL of cyanobacteria in 5 mL of RNAlater solution) stored at –20 °C was subjected to DNA extraction, using the MoBio PowerSoil kit according to the manufacturer's instructions. Barcoded primers S15F (5'-GTGCCAGCMGCCGCGTAA-3') and 806R (5'-GGACTACHVGGGTWTCTAAT-3') and ToughMix PCR (Quanta Biosciences) were used to amplify the V4 region of the bacterial and archaeal 16S rRNA gene.⁴⁶ PCR reactions were run in triplicate with each technical replicate given a different combination of barcodes. Reactions were prepared in triplicate with the following components in each reaction: 1 μM of each primer, 12.5 μL of ToughMix [2×], and 1 μL of extracted DNA (1.39 μg/mL) in a final volume of 25 μL. Amplification parameters were as follows: an initial denaturation at 94 °C for 3 min followed by 35 cycles of 94 °C for 45 s, 50 °C for 60 s, and 72 °C for 90 s with a final extension at 72 °C for 10 min. Reactions were run on a 1.2% agarose gel to assess amplification. Successful triplicate reactions were pooled and cleaned using Agencourt AMPure magnetic beads according to the manufacturer's instructions (Beckman Coulter), DNA concentrations were quantified

using the Invitrogen Qubit dsDNA kit, and all samples were pooled together in equimolar ratios. The pooled samples were assessed for amplicon length and purity on an Agilent Bioanalyzer 2100 and then sequenced using the Illumina MiSeq platform through Oregon State University's Center for Genome Research and Biocomputing (CGRB).

MiSeq sequence data were processed in the QIIME pipeline using MacQIIME v1.9.1. Reads were separated by barcode tags and processed for quality by trimming low-quality bases, discarding short read lengths, and chimeras were filtered out with USEARCH 6.1544 default parameters.⁴⁶ Of the 1379 sequences generated, 410 belonged to a single operational taxonomic unit (OTU), which was far more common than any other sets of sequences generated. The 253 bp derived from the 16S rRNA V4 region of the single OTU described above (GenBank accession MG552780) were aligned using MUSCLE⁴⁷ with 36 other cyanobacterial 16S rRNA V4 region sequences. The generalized time-reversible (GTR) algorithm⁴⁸ was used to construct a maximum likelihood with 1000 bootstrap replicates using the MEGA7 software.⁴⁹ All positions containing gaps were eliminated.

Extraction and Isolation. Approximately 170 g of lyophilized cyanobacterial material was extracted repeatedly with CH₂Cl₂–MeOH (2:1) to produce approximately 10.4 g of an organic extract. The extract was fractionated by successive normal-phase vacuum-liquid chromatography (NPVLC) separations using stepwise gradients of two different solvent systems. Upon Si gel elution with hexanes–EtOAc–MeOH, the 50% EtOAc–MeOH first-tier fraction was reapplied to Si gel using a hexanes–CHCl₃–MeOH solvent system. The resultant second-tier NPVLC fraction (627 mg) that eluted in 10–12% MeOH in CHCl₃ was fractionated further by RP₁₈ CombiFlash chromatography with a stepwise gradient solvent system from 30% to 100% MeOH–H₂O to yield three fractions (30–40%, 40–75%, 75–100%). The 75–100% MeOH (25.3 mg) RP₁₈ fraction inhibited protease activity (at 10 µg/mL) in an assay designed to detect inhibition of the type II secretion system in *V. cholerae* and was chromatographed again by RP₁₈ SPE using the same solvent gradient. The SPE fraction eluting with 70–95% MeOH (8.2 mg) possessed interesting peptide-like ¹H NMR spectroscopic features and LC-MS/MS data that matched with the biologically active parent fraction. This SPE fraction was separated further by RP₁₈ HPLC (35:65 MeCN–H₂O + 0.1% formic acid (FA)), Phenomenex Synergi Hydro 4 µm, 10 × 250 mm, 4.50 mL/min, UV detection at 210 nm) to yield jizanpeptins A (1, 1.0 mg, *t*_R 18.1 min), B (2, 0.4 mg, *t*_R 21.9 min), C (3, 0.6 mg, *t*_R 20.2 min), D (4, 0.3 mg, *t*_R 28.8 min), and E (5, 0.6 mg, *t*_R 25.4 min).

Jizanpeptin A (1): colorless oil; [α]_D²³ –21 (*c* 0.1, MeOH); UV (35% MeCN–H₂O + 0.1% FA) λ_{\max} (log ϵ) 198 (6.16), 210 (5.87), 280 (4.69) nm; ¹H and ¹³C NMR data, see Tables 1 and S1 (Supporting Information); HRTOFMS (ES+) *m/z* 1122.4391 [M + NH₄]⁺ (calcd for C₄₆H₇₃⁷⁹BrN₈O₁₆S, 1122.4387).

Jizanpeptin B (2): colorless oil; [α]_D²³ –18 (*c* 0.1, MeOH); UV (35% MeCN–H₂O + 0.1% FA) λ_{\max} (log ϵ) 198 (6.20), 210 (5.89), 280 (4.70) nm; ¹H and ¹³C NMR data, see Tables 1 and S2 (Supporting Information); HRTOFMS (ES+) *m/z* 1136.4555 [M + NH₄]⁺ (calcd for C₄₇H₇₅⁷⁹BrN₈O₁₆S, 1136.4543).

Jizanpeptin C (3): colorless oil; [α]_D²³ –37 (*c* 0.1, MeOH); UV (35% MeCN–H₂O + 0.1% FA) λ_{\max} (log ϵ) 198 (6.30), 210 (5.99), 280 (4.80) nm; ¹H and ¹³C NMR data, see Tables 1 and S3 (Supporting Information); HRTOFMS (ES+) *m/z* 1136.4558 [M + NH₄]⁺ (calcd for C₄₇H₇₅⁷⁹BrN₈O₁₆S, 1136.4543).

Jizanpeptin D (4): colorless oil; [α]_D²³ –28 (*c* 0.1, MeOH); UV (35% MeCN–H₂O + 0.1% FA) λ_{\max} (log ϵ) 198 (5.82), 210 (5.48), 280 (4.36) nm; ¹H and ¹³C NMR data, see Tables 1 and S4 (Supporting Information); HRTOFMS (ES+) *m/z* 1150.4679 [M + NH₄]⁺ (calcd for C₄₈H₇₇⁷⁹BrN₈O₁₆S, 1150.4700).

Jizanpeptin E (5): colorless oil; [α]_D²³ –14 (*c* 0.1, MeOH); UV (35% MeCN–H₂O + 0.1% FA) λ_{\max} (log ϵ) 198 (6.18), 210 (5.84), 280 (4.66) nm; ¹H and ¹³C NMR data, see Tables 1 and S5 (Supporting Information); HRTOFMS (ES+) *m/z* 1164.4596 [M + NH₄]⁺ (calcd for C₄₇H₇₅⁷⁹BrN₁₀O₁₆S, 1164.4605).

Absolute Configurations of Jizanpeptins A–E (1–5). The absolute configurations of the amino acid residues in jizanpeptins A–E (1–5) were determined using Marfey's method. Approximately 0.2 mg of each of 1–5 were separately hydrolyzed (6 N HCl at 110 °C for 24 h in an oil bath), evaporated to dryness, and reconstituted in 50:50 MeOH–H₂O (100 µL). FDLA solution in acetone (0.1%, 100 µL) and 1 M NaHCO₃ (20 µL, 20 µmol) were added to each hydrolysate and heated to 40 °C for 1 h. The solutions were allowed to cool to room temperature (rt), neutralized with 2 N HCl (10 µL, 20 µmol), and evaporated to dryness. The residues were resuspended in MeCN–H₂O (1:1, 250 µL) and analyzed by RPHPLC (Agilent Zorbax SB-C₃ column, 3.0 × 250 mm, 0.5 mL/min, UV detection at 340 nm) using a linear gradient of 50% MeOH + 0.5% FA; 50% H₂O + 0.5% FA to 90% MeOH + 0.5% FA; 10% H₂O + 0.5% FA over 50 min. The absolute configurations of the amino acids in the hydrolysates of 1–5 were determined by HPLC-based direct comparison with the retention times (*t*_R, min) for Marfey's derivatives of authentic standards (50 µM). *N,O*-Di-Me-L-BrTyr provided by the Luesch laboratory³⁰ was racemized as reported previously¹⁹ to provide both D- and L-standards.

The retention times (min) of the FDLA-derivatized α -amino acids in the hydrolysates of 1 and 2 matched those of L-Thr (12.5; D-Thr, 18.8, L-*allo*-Thr 14.6, D-*allo*-Thr 15.7), L-*allo*-Ile (22.6; D-*allo*-Ile, 33.2), L-Ile (23.6; D-Ile, 34.3), *N,O*-di-Me-L-BrTyr (24.4; *N,O*-di-Me-D-BrTyr, 25.8), D-Val (30.2; L-Val, 20.8), and L-Lys (34.6; D-Lys, 37.6). The retention times (min) of the derivatized amino acids in the hydrolysate of 3 were the same with the exception of L-Val in place of D-Val. The retention times (min) of the derivatized amino acids in the hydrolysate of 4 were the same as those of 1 and 2 with L-Ile in place of D-Val. The retention times (min) of the derivatized amino acids in the hydrolysate of 5 matched 1 and 2 with the exception of L-Arg (9.0; D-Arg 7.3) in place of L-Lys.

Chiral-phase HPLC analysis was used to determine the absolute configurations of the Gac-sulfate and Mgs residues in the five depsipeptides. A portion of the acid hydrolysate of 1–5 (0.1 mg) was reconstituted in H₂O–MeCN prior to chiral-phase HPLC analysis (85:15 2 mM CuSO₄–MeCN; column Phenomenex Chirex 3126 (D), 4.6 × 250 mm, flow 1.0 mL/min, UV detection at 254 nm). The Gac residue in the hydrolysate of 1 eluted with the same retention time (*t*_R, min) as commercial standard R-Gac (5.9) but not that of S-Gac (5.2) (Figures S37–S39, Supporting Information). For 2–5, 80:20 MeOH/10 mM NH₄OAc, pH 5.3 buffer was used with a Chirobiotic TAG column 4.6 × 250 mm, flow rate 0.5 mL/min, UV detection at 210 nm. The acid hydrolysates showed a retention time that matched that of our synthetic R-Mga (6.6 min) but not S-Mga (5.7 min) (Figures S40–S42, Supporting Information).

Synthesis of R- and S-Mga was performed using a slightly modified method to that reported by Luesch et al.¹⁶ Thus, D- or L-serine (50 mg), isoamyl nitrite (141 µL), glacial acetic acid (17.2 µL), MgSO₄ (60 mg), and anhydrous MeOH (1 mL) were placed in a clear glass vial (11 mL) and heated to 110 °C (oil bath) with constant stirring for 4 h. The resulting product was cooled to rt, filtered, and dried under vacuum to yield S-/R- (racemic) or S-Mga, respectively. The observed NMR data for the crude products were in agreement with those reported previously (Figures S43–S45, Supporting Information).⁴⁶

Assignment of the Ahp residue relied on pyridinium chlorochromate (PCC) oxidation of 2, followed by acid hydrolysis and derivatization with FDLA, and comparison with FDLA-derivatized D/L-Glu standards. Approximately 0.1 mg of 2 was dissolved in 100 µL of CH₂Cl₂ and stirred with 2 mg of PCC at rt for 16 h. The reaction was quenched with 200 µL of H₂O. The organic phase was removed, and the aqueous phase washed twice with 500 µL of CH₂Cl₂. The combined organics were dried and subjected to Marfey's method. The Marfey's derivatized oxidation product had a retention time (*t*_R, min) on an RP₁₈ HPLC Synergi Fusion 4.6 × 250 mm column, 1.0 mL/min, UV detection at 340 nm using a linear gradient of 30% MeCN + 0.1% FA; 70% H₂O + 0.1% FA to 70% MeCN + 0.1% FA; 30% H₂O + 0.1% FA over 50 min, matching that of L-Glu (18.4 min) rather than D-Glu (19.2 min).

Vibrio cholerae T2S Inhibition Assay. For all experiments the transformed *V. cholerae* O395 strain (containing the pBBR322 plasmid

bearing the PT2S-lux construct⁵⁰) was grown under laboratory conditions inducing virulence gene expression (LB pH 6.5, 30 °C). Positive controls for the assay included both *V. cholerae* carrying the empty vector pBBR322 (the level of detected bioluminescence is diminished to the background level, LB) and *V. cholerae* grown in the presence of leupeptin, a protease inhibitor. The activity of the protease in the presence of leupeptin is as low as in the cultures of T2S mutants, which averaged 93% reduction in fluorescence.¹⁷ The LB liquid medium required for *V. cholerae* growth was added to each well of the 96-well microtiter plates, after which the test samples were delivered from a sister plate using a semiautomated Sorenson BioScience benchtop pipettor. Cultures of *V. cholerae* were added to the plates using a BioTek plate dispenser. Each plate contained negative and positive controls for the assay as described above, as well as solvent (DMSO) vehicle controls. After incubation in a humid chamber at 30 °C, the turbidity of all cultures was measured because many compounds could inhibit bacterial growth either via the bactericidal or bacteriostatic mechanism of action. Subsequently, the assay was completed by measurement of luminescence (pPT2S-lux activity) and finally addition of the AMC substrate for the protease, followed by measurement of fluorescence in a Synergy HT Multi-Mode microplate reader (BioTek).^{17,50}

Trypsin Assay. Solutions of the trypsin substrate, *N*-benzoyl-L-arginine ethyl ester hydrochloride (BAEE) (0.25 mM), and trypsin (1.0 mg/mL in cold HCl, 1 mM) were prepared in NaH₂PO₄ buffer (67 mM, pH 7.6 at 25 °C) immediately before use. Jizanpeptins A–E (1–5) were reconstituted in 100% MeOH and stock solutions (3 mM) used to generate a dilution series of each compound in MeOH on the day of the experiment, to yield a final concentration range of 3 nM to 10 μM in a 500 μL reaction volume. The substrate BAEE (500 μL) plus a jizanpeptin, or MeOH (blank), was mixed in a quartz cuvette and allowed to equilibrate to 25 °C in a BioSpectrophotometer (Eppendorf). Trypsin (12 μL of 500 units/mL) was then added and mixed rapidly by inversion, and the production of *N*-benzoyl-L-arginine from BAEE was followed by observing the continuous change in absorbance at 253 nm with time. A 5 min reaction time was used to follow and establish the activity of uninhibited trypsin, and a 30 s time interval was used for subsequent spectrophotometric analyses, in which independent reactions were carried out in the presence of fixed concentrations of each test compound (1–5). Trypsin activity was calculated, in the presence and absence of inhibitor, and plotted as BAEE units/mL trypsin, where one BAEE unit is the amount of trypsin needed to produce a change in absorbance (A₂₅₃ nm) of 0.001/min of the substrate BAEE at pH 7.6 at 25 °C. The activities of 1–5 were measured side-by-side on the same day, and the assay was repeated on subsequent days to give a total of three determinations. Concentration–response relationships for all titrations were analyzed using GraphPad Prism software (GraphPad Software Inc.), and IC₅₀ values were derived using nonlinear regression analysis.

Chymotrypsin Assay. Solutions of *N*-benzoyl-L-tyrosine ethyl ester solution (BTEE) (1.18 mM) in Tris HCl buffer (80 mM, pH 7.8 at 25 °C), and chymotrypsin (4 units/mL of chymotrypsin in cold HCl (1 mM)) were prepared immediately before use. Stock solutions of jizanpeptins A–E (1–5) in 100% MeOH were used to generate a dilution series of each compound in MeOH (as above). The substrate solution (BTEE; 233 μL), Tris HCl buffer (80 mM, pH 7.8; 236 μL), CaCl₂ (13.3 μL), and a jizanpeptin or MeOH (blank) were mixed in a quartz cuvette and allowed to equilibrate to 25 °C in a BioSpectrophotometer (Eppendorf). Chymotrypsin (16.7 μL of 4 units/mL) was added last and mixed rapidly by inversion, and the production of *N*-benzoyl-L-tyrosine from BTEE was followed by observing the continuous change in absorbance of 256 nm with time. A 3 min reaction time was used to follow and establish the activity of uninhibited chymotrypsin, and a time interval of 30 s was used for subsequent spectrophotometric analyses. Chymotrypsin activity was calculated, in the presence and absence of inhibitor, and plotted as BTEE units/mL, where one unit of chymotrypsin will hydrolyze 1 μmol of BTEE per minute at pH 7.8 at 25 °C. The activities of 1–5 were measured side-by-side on the same day, and the assay was repeated twice for jizanpeptin C (3) and once over a limited range for

jizanpeptins 1, 2, 4, and 5. Concentration–response relationships were analyzed using GraphPad Prism software (GraphPad Software Inc.), and the IC₅₀ value for jizanpeptin C (3) was derived using nonlinear regression analysis.

Antiproliferative/Cytotoxicity Assays. The antiproliferative/cytotoxic potential of jizanpeptins A–E (1–5) was assessed using a standard 3-(4,5-dimethylthiazolyl-2)-2,5-diphenyltetrazolium bromide (MTT) cell viability assay. All compounds were reconstituted in 100% cell culture-grade DMSO and stored at –20 °C until the day of treatment. Human cancer cells were treated at the same time to expose cells to increasing concentrations (30 nM to 3 μM) of each jizanpeptin (1–5), vehicle (0.1% DMSO), or cytotoxin apratoxin A (30 nM) as a positive control, for 72 h (NCI-H460) or 48 h (HeLa). The final concentration of DMSO on cells was held constant at 0.1% in all experiments. All concentration–response data were analyzed using GraphPad Prism software (GraphPad Software Inc.) with the viability of vehicle-treated cells defined as 100% viability.

■ ASSOCIATED CONTENT

Supporting Information

The Supporting Information is available free of charge on the ACS Publications website at DOI: 10.1021/acs.jnatprod.8b00117.

1D and 2D NMR spectra for jizanpeptins A–E (1–5); mass spectra for 1–5; Marfey's analyses for 1–5; protease inhibition concentration–response profiles for 1–5; analyses of cell viability in NCI-H460 and HeLa cancer cells; phylogenetic alignment tree (PDF)

Table of reported micropeptin-type protease inhibitors with amino acid sequence and biological activity (XLSX)

■ AUTHOR INFORMATION

Corresponding Author

*Tel: +1 541 737 5808. Fax: +1 541 737 3999. E-mail: kerry.mcphail@oregonstate.edu.

ORCID

David A. Gallegos: 0000-0002-5552-8107

Josep Saurí: 0000-0002-2706-2426

Ryan D. Cohen: 0000-0002-3112-6410

Xuemei Wan: 0000-0001-8049-8192

Patrick Videau: 0000-0003-2686-845X

Alec O. Vallota-Eastman: 0000-0002-6453-4680

Lamiaa A. Shaala: 0000-0002-1866-8258

Diaa T. A. Youssef: 0000-0003-2217-4039

R. Thomas Williamson: 0000-0001-7450-3135

Gary E. Martin: 0000-0003-0750-3041

Benjamin Philmus: 0000-0003-2085-0873

Aleksandra E. Sikora: 0000-0001-7977-2596

Jane E. Ishmael: 0000-0003-4574-2801

Kerry L. McPhail: 0000-0003-2076-1002

Notes

The authors declare no competing financial interest.

■ ACKNOWLEDGMENTS

Financial support is gratefully acknowledged from the OSU College of Pharmacy, NIH R15 GM122016-01 (support of D.A.G.), and Oregon Sea Grant under award number NA10OAR4170064 (project number R/BT-52) from the National Oceanic and Atmospheric Administration's National Sea Grant College Program, U.S. Department of Commerce, and by appropriations made by the Oregon state legislature. We thank the Government of Saudi Arabia for permission to make

this collection. We thank S. Huhn and the OSU NMR Facility for support in collection of NMR data. *N,O*-di-Me-L-BrTyr was a kind gift from Dr. H. Luesch.

■ REFERENCES

- (1) Nagarajan, M.; Maruthanayagam, V.; Sundararaman, M. *J. Appl. Toxicol.* **2013**, *33*, 313–349.
- (2) Chlipala, G. E.; Mo, S.; Orjala, J. *Curr. Drug Targets* **2011**, *12*, 1654–1673.
- (3) Salvador-Reyes, L. A.; Luesch, H. *Nat. Prod. Rep.* **2015**, *32*, 478–503.
- (4) Tan, L. T. *Drug Discovery Today* **2013**, *18*, 863–871.
- (5) Williams, M. R.; Nakatsuji, T.; Sanford, J. A.; Vrbanac, A. F.; Gallo, R. L. *J. Invest. Dermatol.* **2017**, *137*, 377–384.
- (6) Lee, H.; Ren, J.; Nocadello, S.; Rice, A. J.; Ojeda, I.; Light, S.; Minasov, G.; Vargas, J.; Nagarathnam, D.; Anderson, W. F.; Johnson, M. E. *Antiviral Res.* **2017**, *139*, 49–58.
- (7) Shin, B.; Park, S. H.; Kim, B. Y.; Jo, S. I.; Lee, S. K.; Shin, J.; Oh, D. C. *J. Nat. Prod.* **2017**, *80*, 2910–2916.
- (8) Piccirillo, E.; Merget, B.; Sottriffer, C. A.; do Amaral, A. T. *J. Comput.-Aided Mol. Des.* **2016**, *30*, 251–270.
- (9) Chen, X.; Yang, K.; Wu, C.; Chen, C.; Hu, C.; Buzovetsky, O.; Wang, Z.; Ji, X.; Xiong, Y.; Yang, H. *Cell Res.* **2016**, *26*, 1260–1263.
- (10) Thornburg, C. C.; Thimmaiah, M.; Shaala, L. A.; Hau, A. M.; Malmo, J. M.; Ishmael, J. E.; Youssef, D. T.; McPhail, K. L. *J. Nat. Prod.* **2011**, *74*, 1677–1685.
- (11) Thornburg, C. C.; Cowley, E. S.; Sikorska, J.; Shaala, L. A.; Ishmael, J. E.; Youssef, D. T.; McPhail, K. L. *J. Nat. Prod.* **2013**, *76*, 1781–1788.
- (12) Shaala, L. A.; Youssef, D. T. A.; McPhail, K. L.; Elbandy, M. *Phytochem. Lett.* **2013**, *6*, 183–188.
- (13) Lopez, J. A. V.; Al-Lihaibi, S. S.; Alarif, W. M.; Abdel-Lateff, A.; Nogata, Y.; Washio, K.; Morikawa, M.; Okino, T. *J. Nat. Prod.* **2016**, *79*, 1213–1218.
- (14) Pavlik, C. M.; Wong, C. Y. B.; Ononye, S.; Lopez, D. D.; Engene, N.; McPhail, K. L.; Gerwick, W. H.; Balunas, M. J. *J. Nat. Prod.* **2013**, *76*, 2026–2033.
- (15) Choi, H.; Pereira, A. R.; Cao, Z.; Shuman, C. F.; Engene, N.; Byrum, T.; Matainaho, T.; Murray, T. F.; Mangoni, A.; Gerwick, W. H. *J. Nat. Prod.* **2010**, *73*, 1411–1421.
- (16) Tran, N.; Zielke, R. A.; Vining, O. B.; Azevedo, M. D.; Armstrong, D. J.; Banowetz, G. M.; McPhail, K. L.; Sikora, A. E. *J. Biomol. Screening* **2013**, *18*, 921–929.
- (17) Sikora, A. E.; Zielke, R. A.; Lawrence, D. A.; Andrews, P. C.; Sandkvist, M. *J. Biol. Chem.* **2011**, *286*, 16555–16566.
- (18) Sikora, A. E.; Beyhan, S.; Bagdasarian, M.; Yildiz, F. H.; Sandkvist, M. *J. Bacteriol.* **2009**, *191*, 5398–5408.
- (19) Linington, R. G.; Edwards, D. J.; Shuman, C. F.; McPhail, K. L.; Matainaho, T.; Gerwick, W. H. *J. Nat. Prod.* **2008**, *71*, 22–27.
- (20) Elkobi-Peer, S.; Carmeli, S. *Mar. Drugs* **2015**, *13*, 2347–2375.
- (21) Salvador, L. A.; Taori, K.; Biggs, J. S.; Jakoncic, J.; Ostrov, D. A.; Paul, V. J.; Luesch, H. *J. Med. Chem.* **2013**, *56*, 1276–1290.
- (22) Gesner-Apter, S.; Carmeli, S. *J. Nat. Prod.* **2009**, *72*, 1429–1436.
- (23) Itou, Y.; Ishida, K.; Shin, H. J.; Murakami, M. *Tetrahedron* **1999**, *55*, 6871–6882.
- (24) Okumura, H. S.; Philmus, B.; Portmann, C.; Hemscheidt, T. K. *J. Nat. Prod.* **2009**, *72*, 172–176.
- (25) Zafrir, E.; Carmeli, S. *J. Nat. Prod.* **2010**, *73*, 352–358.
- (26) Zafrir-Ilan, E.; Carmeli, S. *Tetrahedron Lett.* **2010**, *51*, 6602–6604.
- (27) Vegman, M.; Carmeli, S. *Tetrahedron* **2013**, *69*, 10108–10115.
- (28) Carroll, A. R.; Pierens, G. K.; Fechner, G.; De Almeida Leone, P.; Ngo, A.; Simpson, M.; Hyde, E.; Hooper, J. N.; Bostrom, S. L.; Musil, D.; Quinn, R. J. *J. Am. Chem. Soc.* **2002**, *124*, 13340–13341.
- (29) Taori, K.; Paul, V. J.; Luesch, H. *J. Nat. Prod.* **2008**, *71*, 1625–1629.
- (30) Matthew, S.; Ross, C.; Paul, V. J.; Luesch, H. *Tetrahedron* **2008**, *64*, 4081–4089.
- (31) Kwan, J. C.; Taori, K.; Paul, V. J.; Luesch, H. *Mar. Drugs* **2009**, *7*, 528–538.
- (32) Plaza, A.; Bewley, C. A. *J. Org. Chem.* **2006**, *71*, 6898–6907.
- (33) Pettit, G. R.; Kamano, Y.; Herald, C. L.; Dufresne, C.; Cerny, R. L.; Herald, D. L.; Schmidt, J. M.; Kizu, H. *J. Am. Chem. Soc.* **1989**, *111*, 5015–5017.
- (34) Matthew, S.; Ross, C.; Rocca, J. R.; Paul, V. J.; Luesch, H. *J. Nat. Prod.* **2007**, *70*, 124–127.
- (35) Druga, B.; Turko, P.; Spaak, P.; Pomati, F. *Environ. Sci. Technol.* **2016**, *50*, 3416–3424.
- (36) Stolze, S. C.; Meltzer, M.; Ehrmann, M.; Kaiser, M. *ChemBioChem* **2013**, *14*, 1301–1308.
- (37) Gademann, K.; Portmann, C.; Blom, J. F.; Zeder, M.; Juttner, F. *J. Nat. Prod.* **2010**, *73*, 980–984.
- (38) Okano, T.; Sano, T.; Kaya, K. *Tetrahedron Lett.* **1999**, *40*, 2379–2382.
- (39) Sikora, A. E. *PLoS Pathog.* **2013**, *9*, e1003126.
- (40) Gadwal, S.; Korotkov, K. V.; Delarosa, J. R.; Hol, W. G.; Sandkvist, M. *J. Biol. Chem.* **2014**, *289*, 8288–8298.
- (41) Hatzios, S. K.; Abel, S.; Martell, J.; Hubbard, T.; Sasabe, J.; Munera, D.; Clark, L.; Bachovchin, D. A.; Qadri, F.; Ryan, E. T.; Davis, B. M.; Weerapana, E.; Waldor, M. K. *Nat. Chem. Biol.* **2016**, *12*, 268–274.
- (42) Mondal, A.; Tapader, R.; Chatterjee, N. S.; Ghosh, A.; Sinha, R.; Koley, H.; Saha, D. R.; Chakrabarti, M. K.; Wai, S. N.; Pal, A. *Infect. Immun.* **2016**, *84*, 1478–1490.
- (43) Ruiz-Perez, F.; Nataro, J. P. *Cell. Mol. Life Sci.* **2014**, *71*, 745–770.
- (44) Anas, A. R. J.; Nakajima, A.; Naruse, C.; Tone, M.; Asukabe, H.; Harada, K.-i. *Mar. Drugs* **2016**, *14*, 7.
- (45) Tan, X.; Bertoni, C.; Qin, L.; Furio, L.; El Amri, C.; Hovnanian, A.; Reboud-Ravaux, M.; Villoutreix, B. O. *Eur. J. Med. Chem.* **2013**, *70*, 661–668.
- (46) Caporaso, J. G.; Kuczynski, J.; Stombaugh, J.; Bittinger, K.; Bushman, F. D.; Costello, E. K.; Fierer, N.; Pena, A. G.; Goodrich, J. K.; Gordon, J. I.; Huttley, G. A.; Kelley, S. T.; Knights, D.; Koenig, J. E.; Ley, R. E.; Lozupone, C. A.; McDonald, D.; Muegge, B. D.; Pirrung, M.; Reeder, J.; Sevinsky, J. R.; Turnbaugh, P. J.; Walters, W. A.; Widmann, J.; Yatsunenko, T.; Zaneveld, J.; Knight, R. *Nat. Methods* **2010**, *7*, 335–336.
- (47) Edgar, R. C. *Nucleic Acids Res.* **2004**, *32*, 1792–1797.
- (48) Tavaré, S. In *Lectures on Mathematics in the Life Sciences*; Miura, R. M., Ed.; American Mathematical Society: Providence, RI, 1986; Vol. 17, pp 57–86.
- (49) Kumar, S.; Stecher, G.; Tamura, K. *Mol. Biol. Evol.* **2016**, *33*, 1870–1874.
- (50) Zielke, R. A.; Simmons, R. S.; Park, B. R.; Nonogaki, M.; Emerson, S.; Sikora, A. E. *Infect. Immun.* **2014**, *82*, 2788–2801.